



American Society of
Mechanical Engineers

ASME Accepted Manuscript Repository

Institutional Repository Cover Sheet

Marina

Braun-Unkhoff

First

Last

ASME Paper

Title: An Investigation of Combustion Properties of Butanol and its Potential for Power Generation

Authors:

Torsten Methling, Sandra Richter, Trupti Kathrotia, Marina Braun-Unkhoff*,
Clemens Naumann, Uwe Riedel

ASME Journal Title: J. Eng. Gas Turbines Power

Volume/Issue 140(9) Date of Publication (VOR* Online) Jun 15, 2018

ASME Digital Collection URL: <http://gasturbinespower.asmedigitalcollection.asme.org/article.aspx?articleid=2676913>

DOI: 10.1115/1.4039731

*VOR (version of record)

An Investigation of Combustion Properties of Butanol and its Potential for Power Generation

Torsten Methling, Sandra Richter, Trupti Kathrotia,

Marina Braun-Unkhoff*, Clemens Naumann, Uwe Riedel

German Aerospace Center (DLR)

Institute of Combustion Technology

Pfaffenwaldring 38-40, 70569 Stuttgart, Germany

E-Mail: Marina.Braun-Unkhoff@dlr.de

ABSTRACT

Over the last years, global concerns about energy security and climate change have resulted in many efforts focusing on the potential utilization of non-petroleum-based, *i.e.* bio-derived, fuels. In this context, *n*-butanol has recently received high attention because it can be produced sustainably. A comprehensive knowledge about its combustion properties is inevitable to ensure an efficient and smart use of *n*-butanol if selected as a future energy carrier. In the present work, two major combustion characteristics, here laminar flame speeds applying the cone-angle method and ignition delay times applying the shock tube technique, have been studied, experimentally and by modeling exploiting detailed chemical kinetic reaction models, at ambient and elevated pressures. The in-house reaction model was constructed applying the RMG-method. A linear transformation method recently developed, linTM, was exploited to generate a reduced reaction model needed for an efficient, comprehensive parametric study of the combustion behavior of *n*-butanol-hydrocarbon mixtures. All experimental data were found to agree with the model predictions of the in-house reaction model, for all temperatures, pressures, and fuel-air ratios. On the other hand, calculations using reaction models from the open literature mostly overpredict the measured ignition delay times by about a factor of two. The results are compared to those of ethanol, with ignition delay times very similar and laminar flame speeds of *n*-butanol slightly lower, at atmospheric pressure.

Keywords: alternative fuels, butanol, laminar flame speed, ignition delay time, reaction mechanism.

INTRODUCTION

Demands of energy will increase worldwide, while fossil resources are depleted. To address this challenge, many efforts have been devoted to raise efficiencies of current combustion concepts and to new approaches for gas turbines. The use of alternative and renewable energy resources is attracting much interest, to counteract climate change connected to the burning of fossil fuels. Moreover, improvements in fuel flexibility are a prerequisite to meet the challenge of a more sustainable production of power in the near future.

Currently, it is discussed to which extent future energy demands can be satisfied by biomass and by-products, also for decentralized power generation, *e.g.* in micro gas turbines. However, in order to ensure low emission levels at the same time, new concepts and new unconventional fuels require a re-investigation of at least the burner and also the gas turbine itself. This will allow to ensure a safe operation and a maximum range of tolerating variations of fuel composition and conditions (fuel flexibility, load flexibility).

Within this context, alcohols have gained high interest as alternative fuels [1-2]. Recently, butanol has attracted much attention as this higher alcohol (C4) can be produced from sustainable sources, *e.g.* via fermentation of sugars, starch and other biomass including 2nd generation and through pyrolysis and reformulation of biomass [3]. Thus, an increased use of butanol, a so-called “next-generation” alcohol, is foreseen.

Butanol might play a role as an alternative transport fuel [4-6]. Compared to ethanol, butanol offers better physico-chemical properties, *e.g.* a higher energy density and cetane number, a lower hygroscopicity meaning a reduced corrosiveness and a lower vapor pressure, actually much closer to gasoline, meaning a lower volatility and reduced evaporative emissions [6]. Moreover, an improvement in local air quality is expected based on reduced emissions of particles and soot due to the fuel-bound oxygen [7] counteracting particle formation. For these reasons, it is not surprising that recently *n*-butanol has been certified by ASTM International for use as automotive spark-ignition engine fuel up to a 12.5% blending rate [8]. This new standard also includes 2-butanol and *iso*-butanol.

Furthermore, its potential for power generation is also of interest: Burning in gas turbines, decentralized (micro gas turbines) or centralized gas turbines, neat or co-fired with liquid fuel like diesel, gasoline, or kerosene and gaseous fuels like natural gas and biogas [9-10]. Within this context, micro gas turbines offer several advantages over conventional gas engines, such as high fuel flexibility with a broad range of liquid and gaseous fuels and substantially lower pollutant emissions. Their on-site combined heat and power production are expected to play a more prominent role in the near future, in particular for decentralized power generation [11-12]. Also, a much better electrical efficiency of small gas turbines can be reached by following the concept of a hybrid power plant [12].

Detailed knowledge of fundamental combustion properties *e.g.* flame speed and auto ignition is a prerequisite to enable a reliable and safe operation when using these advanced (bio-) fuels. An overview of these properties available from literature for *n*-butanol is given in Tables 1-2. Concerning laminar flame speed, data are available in a restricted fuel-air range and at preheat temperatures almost not higher than 428 K (Fig. 1).

Chemical kinetic modeling has become an important tool for interpreting and understanding the combustion phenomena observed and also for their prediction if a reaction scheme validated for the relevant parameters exists. Such validated chemical kinetic reaction models allow a more sophisticated design of burners as well as of the burner's combustion chamber, when coupled to CFD codes.

In the present work, up to four detailed reaction models will be used for the description of the oxidation of *n*-butanol focusing on two major combustion properties: (i) laminar flame speed data, at ambient and elevated pressures; and (ii) ignition delay times measured at different pressures, for stoichiometric mixtures. Recently, we have reported about the use of ethanol for power generation, neat or co-fired with natural gas [9]. These results allow a comparison between these two major combustion properties of the two alcohols.

EXPERIMENTAL AND MODELING-APPROACH

To best optimize fuel-air mixture application in practical combustors, their fundamental combustion characteristics must be well understood. In the present work a combined experimental and modeling approach is followed.

First, two types of measurements were performed:

- (i) Ignition delay times τ of diluted *n*-butanol-air mixtures (with argon (Ar) replacing nitrogen (N₂)) applying the shock tube method, for a stoichiometric fuel-air ratio, $\phi = 1.0$, at three pressures, $p = 1$ bar, 4 bar, and 16 bar, and temperatures between about 950 and 1800 K;
- (ii) Burning velocities S_u of *n*-butanol-air mixtures making use of the cone angle method, for three different pressures, $p = 1$ bar, 3 bar, and 6 bar, at a preheat temperature $T = 473$ K, and for (fuel) equivalence ratios ϕ ranging between 0.50 and 2.0 (1 bar), 0.6 and 1.9 (3 bar), and 0.7 and 1.6 (6 bar), respectively.

Details of the mixtures are summarized in Table 3.

Then, the measured data are compared with predictions of up to four detailed chemical kinetic reaction models, an in-house model and three public-domain models [30, 32-37]. Main features of the reaction models are summarized in Table 4.

Computer simulations of the laminar premixed flames were performed with the open-source software Cantera [38] assuming a free flame. For the simulations, the multi-component diffusion model and thermo-diffusion were considered. For the involved species, transport data were taken from Ref. [39] and thermodynamical data from Ref. [40]. Mesh points were refined to achieve equal solution tolerance; the refine criteria “slope” and “curve” were set to 0.1 leading to about 170 mesh points. The calculation of ignition delay times was obtained by using the Chemical Workbench by Kintech Lab [41]; for details, see [10, 42].

MODELING

The main features of the reaction models used to predict ignition delay times and burning velocities of the mixtures determined in the present work are given in Table 4.

Three public-domain detailed reaction models were used: (i) the Black *et al.* model [30] developed for describing the ignition behavior of *n*-butanol mixtures; (ii) the reaction model from POLIMI [32] shown to describe the combustion behavior of small alcohols; and (iii) the very detailed reaction model from Sarathy *et al.* [33].

Furthermore, an in-house reaction model was used, in a detailed and in a reduced version. This in-house reaction model is consisting of two parts: (1) the detailed sub reaction model for *n*-butanol comprising 66 species and 3749 elementary reactions; this sub model has been constructed using an open-source rule-based reaction model generation software (RMG) developed at MIT [43], for further information see [2]; (2) the primary reference fuel (PRF) sub model with the model components selected *iso*-octane and *n*-heptane (90:10 vol%) representing a gasoline, comprising 115 species and 818 reactions, taken from an existing in-house DLR mechanism [44]. In the present work, both of these sub models are combined in order to be able to predict PRF mixtures with *n*-butanol added. The combined detailed reaction model consists of 181 species and 4567 reactions (Table 4).

With the detailed reaction model as a starting point, a reduced version was elaborated in order to make predictive calculations more effective, with respect to the large parameter range often needed to be addressed, in particular with respect to time consuming multi-dimensional CFD calculations. Therefore, subsequently, a global sensitivity analysis of the automatically generated reaction mechanism was performed by applying the linear transformation model (linTM) [45] developed recently. This approach allows to reduce the size of a mechanism, in particular the number of species, thus enabling its efficient use in CFD simulations. For details, refer to Methling *et al.* [45].

Utilizing linTM, the influence on the shape of concentration time profiles by rate coefficient parameters is quantified, *e.g.* by means of maximum concentration as target points for an optimization process. To select the target concentration profiles for the global sensitivity analysis, homogeneous reactor simulations (adiabatic, isobaric) were performed with Cantera [38] and using the generated full reaction mechanism. The fuel mixture in the simulations was 60 mol% PRF90, 20 mol% *n*-butanol and 20 mol% *n*-propanol. The oxidizer was a mixture of O₂ and N₂ (replacing air) as well as Ar to account for the dilution of the mixtures. Simulations were performed for pressures $p = 1$ bar, 4 bar, and 16 bar. For each pressure, the simulations were performed at $T = 1000$ K, 1700 K, and 2400 K. Concentration profiles of each simulation were selected as target concentration profiles when their maximum mole fraction was at least 0.005.

Figure 2 shows the global sensitivity coefficients S_r of the 10 most sensitive reactions, which were normalized by the maximum sensitivity coefficient $S_{r,max}$. Reactions with a normalized global sensitivity coefficient below 0.06% were skipped (reduced). Besides the chain-branching reaction $H+O_2 \leftrightarrow OH+O$ identified as the most important one, reactions with CO/HCO involved as well as those included in the HO_2/H_2O_2 system are among the most important ones. Furthermore, methyl (CH_3) reactions are also of major influence, in addition to thermal decomposition and H-atom abstraction of *iso*-octane (as the major component of the primary reference fuel).

The reduced DLR in-house reaction mechanism contains 133 species and 1182 reactions (see Table 4).

EXPERIMENTAL

To investigate the combustion properties of *n*-butanol, ignition delay times and laminar burning velocities were measured. An overview of the measurements performed is given in Table 3, with the composition of the fuel-air mixtures studied included.

All experiments on ignition delay times were performed applying the shock tube method [9-10, 42, 46]; burning velocities were performed in our burner test rig [47-50] applying the cone angle method [51-52].

Measurement of the burning velocity

The measurements were done at a preheat temperature of $T = 473$ K, at pressures of $p = 1, 3,$ and 6 bar and for a broad range in the equivalence ratios ϕ . First, the experimental setup is described, and then the detection method (cone angle method) applied for determining burning velocities.

The experimental setup

The burner system used was designed for measuring burning velocities of liquid fuels as recently reported in studies on alternative jet fuels including kerosene as a reference fuel [47-50]. The experimental setup as presented schematically in Fig. 3 consists of three main parts: (i) the preparation of the fuel-air mixture; (ii) the burner itself with the nozzle; and (iii) the detection and evaluation system.

For the preparation of the fuel-air mixture, first the fuel (in this case *n*-butanol, AppliChem 99% min.) was vaporized, mixed with a preheated nitrogen-stream and adjusted to the set temperature T of 473 K. In a second, homogenizing step, the oxygen was added so that the ratio between nitrogen and oxygen amounts to 79:21 (N₂:O₂) to simulate air. The flow rates of the fluids were controlled by a HPLC-pump (type LC-20AD, Shimadzu) in the case of *n*-butanol and by calibrated mass flow controllers (Bronkhorst, type F-111B) for N₂ (Linde, 99.999%) and O₂ (Linde, 99.95%), respectively.

Premixed conical-shaped flames have been stabilized above flame holders with contracting nozzles of different diameters and by the use of a coflow, to widen the range of flames to be investigated. In detail, the following nozzles with different outlet diameters were used: 8 mm ($p = 1$ bar, $\varphi < 1.4$), 6 mm ($p = 1$ bar, $\varphi \geq 1.4$), 4 mm ($p = 3$ bar, all φ), and 3 mm ($p = 6$ bar, all φ). As coflow gases, air was used for rich flames and a mixture of 5 % CH₄, 5 % H₂, and 90 % N₂ for lean flames, respectively.

The cone angle method

Laminar premixed burning velocities S_u were obtained by the cone angle method as described in [51-52]. According to Fig. 4 the values of S_u were calculated from the visible cone angles α and the velocities v_u of the unburned gas (Eq. 1). The velocity v_u is based on the nozzle's diameter and the volumetric flow rate. For the determination of the cone angle, pictures of the flames were recorded with a CCD-camera (type Imager Intense, LaVision).

$$S_u = v_u \cdot \sin \alpha \quad (\text{Eq. 1})$$

The uncertainties, resulting from the accuracies of the mass flow controllers, the cone angle detection, and the treatment of the fuel as ideal gas, were estimated depending on the pressure and the fuel-air ratio; they increase with increasing pressure and φ -difference to stoichiometric conditions ($\varphi = 1.0$).

Typical examples of *n*-butanol-air flames stabilized are given in Fig. 5. The overall uncertainty of the current experiments with respect to the determination of the burning velocities is estimated to be up to about $\pm 10\%$ at

atmospheric pressure, with up to about $\pm 15\%$ for high fuel-air ratios ($\phi > 1.6$), and even more, with up to about $\pm 25\%$ at high pressures and high fuel-air ratios ($p = 6$ bar, $\phi > 1.2$). For a more detailed discussion, see [10].

Measurement of the ignition delay

The measurements were done at a preheat temperature of $T = 473$ K, at pressures of $p = 1, 3,$ and 6 bar and for a broad range in the equivalence ratios ϕ . First, the experimental setup is described, and then the detection method (cone angle method) applied for determining burning velocities.

The experimental setup

The experiments were carried out in a high pressure shock tube with an internal diameter of 98.2 mm [42]. It is divided by two aluminium diaphragms into a driver section of 5.18 m, a small intermediate volume and a driven section of 11.12 m in length. The driven section can be pumped down to pressures below 10^{-6} mbar by a turbomolecular pump. Gas mixtures were prepared manometrically in a 140 l stainless steel storage vessel, which is heated to 80 °C and evacuated using a separate turbomolecular pump to pressures below 10^{-6} mbar. The mixture is prepared by injecting *n*-butanol (Sigma Aldrich 99.8%) with a syringe directly into the evacuated vessel. Pressure and weight of the injected fuel are controlled before adding oxygen (Linde, 99.9999%) and Argon (Linde, 99.9999%).

The shock speed was measured over three 20 cm intervals using four piezo-electric pressure gauges. The temperature and pressure behind the reflected shock wave were computed from the measured incident shock speed and the speed attenuation using a one-dimensional shock model. The estimated uncertainty in reflected shock temperature is less than ± 10 K in the temperature range of our measurements.

The ignition was observed by measuring pressure profiles with piezo-electric gauges (PCB® 113A24 and Kistler® 603B) located at a distance of 1 cm to the end flange. The PCB® gauge was shielded by 1 mm polyimide to reduce heat transfer. Also, the OH*-emission at 308 nm and the CH*-emission at 431 nm were selected by narrow band pass filters (Hugo Anders, FWHM = 5 nm) and measured with photomultipliers (Hamamatsu R3896) and amplified by logarithmic amplifiers (Femto HLVA100). All ignition delay time values were determined by

measuring the time difference between the initiation of the system by the reflected shock wave at the end plate and the occurrence of the CH* maximum (Fig. 6) as this represents an appropriate indicator for simulations.

The experimental setup used in this study allows measurements of ignition delay times for observation times up to 8 ms depending on temperature. Impedance matching at the contact surface was achieved by blending the helium driver gas with argon using two mass flow controllers (Bronkhorst). Due to the attenuation of the reflected shock wave, a post-shock compression increased the initially constant pressure after about 4 ms, increasing the temperature of the mixture and thus accelerating ignition. This facility dependent effect has been quantified and a pressure profile was derived with non-reactive mixtures, in detail with no fuel, to be used when modelling the ignition delay time data as mentioned above.

RESULTS AND DISCUSSION

The comparison between measured and predicted data will be presented. First, laminar burning velocities and calculated laminar flame speed data of *n*-butanol-air mixtures will be discussed for pressures up to 6 bar (Fig. 7). Then, the results on ignition delay time data obtained for up to 16 bar will be presented (Figs. 8-9) exploiting further reaction models taken from literature and compared with ethanol auto ignition data.

Burning velocity

The comparison between measured burning velocities (full symbols) and calculated flame speeds (open symbols, curves) of *n*-butanol-air mixtures at several pressures is given in Fig. 7.

A very good agreement between measured and calculated data exists (Fig. 7) for both the full and the reduced reaction mechanism. The DLR reaction models succeed in predicting the main features (shape, trend, peak position) as well as the pressure dependence. Even more interesting, the specific values of the burning velocity S_u are also matched, in particular in the fuel-lean and slightly fuel-rich regime. The peak position occurring at a ϕ value of about 1.10 is slightly overpredicted, by about 5%, at $p = 1$ bar and predicted with an excellent agreement at higher pressures.

The reaction models taken from literature do not perform better when compared to the in-house reaction model. For example, in the fuel-lean regime, the measured data are overpredicted by the POLIMI model; in the fuel-rich regime, data are underpredicted by POLIMI and Sarathy models. The Black *et al.* model has a good performance except at $p = 6$ bar.

At $p = 1$ bar, laminar premixed flames were stabilized in a fuel-air range φ from 0.5 to 2.0; at higher pressures, this range was slightly reduced, to about $\varphi = 1.7$ at $p = 6$ bar. It is obvious that the burning velocities decrease with increasing pressure (Fig. 7, bottom right); all curves have their maximum at a fuel-air ratio of $\varphi = 1.1$. In detail, the maximum S_u -values are determined at $(91 \pm 2.1) \text{ cm s}^{-1}$ @ $p = 1$ bar, $(71 \pm 3.7) \text{ cm s}^{-1}$ @ $p = 3$ bar, and $(58 \pm 4.0) \text{ cm s}^{-1}$ @ $p = 6$ bar, respectively. Increasing pressure results in a broader shape of the profile. As a result, the differences between the S_u -values identified at the same φ for the different pressures become smaller or vanish nearly completely, with increasing distance from the maxima (peak position).

Error bars of the experimentally obtained S_u -values are given in Fig. 7, derived from the maximum error. The uncertainties in determining the equivalence ratio φ (abscissa) result mainly from the consideration of *n*-butanol as ideal gas after vaporization besides the calibration error of the O_2 mass flow controller. Thus, since in the fuel-rich regime the fuel's fraction is higher than on the lean side, the uncertainties rise with increasing φ -values. Of course, the uncertainties in the burning velocity (ordinate) are likewise influenced by the gas flow due to the dependence on the flow speed (see Eq. 1); however, the deviation of the cone angle detection due to the variation of the flame cone is of much greater influence.

The kind of the uncertainties and their effects depend on the fuel-air ratio. In a fuel-air regime between $0.9 \leq \varphi \leq 1.3$ a constant flame is easy to stabilize. With the φ -value becoming smaller than about 0.9, an even slight pressure fluctuation may lead to small changes in the height of the conical-shaped flame affecting in turn the cone angle. On the fuel-rich side, the flame cone becomes more and more unstable with increasing φ -value; this results in a disturbed flame cone not allowing the determination of the value of the burning velocity any more.

To the best of our knowledge, no data on butanol and ethanol flame speeds are available for the preheat temperature used ($T = 473$ K); see Fig. 1 and Table 1. From literature, data on premixed laminar ethanol- and butanol-air flames are available for $T = 393$ K at atmospheric pressure [19] and, for $T = 423$ K, at higher pressure as well, $p = 1, 3, 5,$ and 10 bar, [22]. At atmospheric pressure, ethanol flame speeds are slightly larger than those of n -butanol, by about 8% at the maximum value; for higher pressures, they are very similar. This is in agreement with the results on n -butanol in the present work.

Ignition delay times

Ignition delay times of fuel-oxygen-argon mixtures ($\phi = 1.0, [\text{O}_2] / [\text{Ar}] = 21\text{vol}\% / 79\text{vol}\%$) were measured at a dilution of 1:5 (20% mixture-80% Ar) at ambient and elevated pressures, *i.e.* around $p = 1, 4,$ and 16 bar; see Table 3. Measured ignition delay times ranged between 30 and 8000 μs , depending on temperature and pressure (Fig. 8, symbols).

The data were compared to predictions using the Chemkin II package [41] and up to four reaction models: three models taken from literature, *i.e.* the Black *et al.* model [30], the POLIMI model [32], and the Sarathy *et al.* model [33], as well as the in-house reaction model, a detailed and a reduced one (Table 4). Calculations were performed for an enlarged temperature range to depict the trend of the prediction of a specific model. All calculated ignition delay time data obtained with the full and the reduced DLR model were practically identical; results given are those obtained with the full model.

The measured ignition delay times are matched excellently by the predicted data exploiting the DLR model (Fig. 8). The temperature and the pressure dependence are both captured. The non-linear dependence of the ignition delay time data with decreasing temperature is described well by the DLR model. For high initial pressures ($p = 4$ and 16 bar), a pressure profile $p = p(t)$ had to be applied for reasons described above: Due to gas dynamic effects mainly caused by the attenuation of the reflected shock wave due to boundary layer interaction, an increase in pressure and thus temperature results, even in the case of no heat release by the shock heated system. The onset is not caused by the so-called NTC (negative temperature coefficient) regime. With higher pressure, the beginning of the non-linear behavior occurs at higher temperatures. The DLR model predicts this effect correctly.

A reasonable agreement between measured and predicted ignition delay time data is seen when using the reaction models taken from literature (Fig. 8). Even at ambient pressure and in the high temperature regime, only the POLIMI model gives a good agreement with the measured data, whereas the Sarathy and the Black models both overpredict the measured data by about a factor of two. At lower temperatures, all three models overestimate the experimental ignition delay times: POLIMI > Black > Sarathy > DLR. A similar picture is seen for higher pressures, $p = 4$ bar and $p = 16$ bar.

No direct comparison between ignition delay time data measured here and those given in Table 2 is possible, due to the different gas mixtures used (diluent used (Ar), dilution 1:5)

The comparison between measured and predicted ignition delay times of *n*-butanol and ethanol [9] as fuels is enabled from Fig. 8 and Fig. 9. Obviously, the alcohols have a very similar ignition behavior. In addition, the predictions show a similar trend when compared to ethanol as fuel.

With linTM, specific sensitivities $S_{r,j}$ for the time coordinate of the maximum of the CH profile (indicator for ignition delay time) were determined (Fig. 10). For the variation of $k(T)$ —required to determine $S_{r,j} - \Delta \ln(k_{\max}(T_m))$ was set to 0.01 at the temperatures T_m 298 K, 666.7 K, and 2000); for details, see [45].

The ignition delay times are most sensitive to the kinetics of the chain branching reaction $\text{H} + \text{O}_2 \leftrightarrow \text{OH} + \text{O}$ followed by reactions pertaining to the sub systems of HCO and HO_2 , respectively. Many H-abstraction reactions of *n*-butanol, with H atoms and OH radicals involved, besides methyl (CH_3) radicals, are identified to be of major importance, too. With increasing pressure, ignition delay times are more sensitive to OH-abstraction reactions, in particular those with *n*-butanol. Besides, the influence of chain-termination reactions, e.g. $2\text{CH}_3(+\text{M}) \leftrightarrow \text{C}_2\text{H}_6$ and $\text{OH} + \text{HO}_2 \leftrightarrow \text{H}_2\text{O} + \text{O}_2$, is increased.

These results reflect the need of using accurate HO₂ and HCO sub systems, besides the *n*-butanol sub system (initiation reactions) in order to describe correctly the ignition behavior of *n*-butanol-oxidizer mixtures in the whole parameter range.

SUMMARY AND CONCLUSIONS

Two major combustion characteristics, *here* laminar flame speeds and ignition delay times, of *n*-butanol-air mixtures have been studied experimentally and by modeling using detailed chemical kinetic reaction models. The newly developed in-house reaction model was constructed applying the RMG-method described in literature using another in-house reaction model, for the fuels *n*-heptane and *iso*-octane only, as seed mechanism. A linear transformation method, linTM, was exploited to generate a reduced reaction model needed for an efficient, comprehensive parametric study of the combustion behavior of *n*-butanol/hydrocarbon mixtures.

Laminar burning velocities of *n*-butanol-air mixtures were stabilized at $p = 1, 3,$ and 6 bar at $T = 473$ K for fuel-air ratios ranging between $0.5 \leq \varphi \leq 1.9$. Ignition delay time data were determined for $\varphi = 1$ at $p = 1, 4,$ and 16 bar and temperatures between about 950 and 1700 K. The onset of the non-linear dependency of the ignition delay time data with temperature was attributed to gas-dynamic effects.

All experimental data were in very good agreement with the model predictions of the in-house reaction model, for all temperatures, pressures, and fuel-air ratios. Calculations by public reaction models used for the ignition behavior overpredict the measured data by about a factor of two.

The findings were discussed to those of ethanol as fuel, with ignition delay times very similar, and laminar flame speeds of *n*-butanol slightly lower than at atmospheric pressure. Thus, with respect to fundamental combustion characteristics, no major modifications are foreseen when operating a (micro) gas turbine either with ethanol or butanol (fuel flexibility).

The results of the present work contribute to a more efficient and a more reliable use of mixtures with *n*-butanol involved, expected to become important as a fuel because of the increasing efforts to replace crude-oil-based fuels

by renewable fuels, preferably bio-fuels. Further investigations will comprise measurements of ignition delay times at fuel-lean and fuel-rich mixtures, besides further butanol isomers, and blends with gasoline and diesel as well as their modeling fuels, *e.g.* PRF.

Acknowledgments

We thank N. Ackermann for his help in the experimental setup and S.L. Duran Estevez, Th. Kick, J. Dembowski, and J. Herzler for supporting the experiments. The assistance of M. Nicolae in ignition delay time calculations is acknowledged.

Nomenclature

p	Pressure
t	Time
S_u	Laminar flame speed
S_r	Sensitivity coefficient
v	Velocity of gas mixture

Greek letters

α	Cone angle
λ	Wavelength
φ	Fuel equivalence ratio
τ	Ignition delay time

Subscripts

0	initial
l	laminar
ign	Ignition
u	unburnt

References

- [1] Sarathy S.M., Oßwald P., Hansen N., Kohse-Höinghaus K., 2014: “*Alcohol combustion chemistry*”, Progr. Energy Combust. Sci. 44, 40-102.
- [2] Köhler M., Kathrotia T., Oßwald P., Fischer-Tammer M.L., Moshhammer K., Riedel U., 2015: “*1-, 2- and 3-Pentanol combustion in laminar hydrogen flames – A comparative experimental and modeling study*”, Combust. Flame 162, 3197-3209.
- [3] Tao L., Aden A., He X., Tan E.C.D., Zhang M., Zigler B.T., McCormick R.L., 2013: “*Techno-Economic Analysis and Life-Cycle Assessment of Cellulosic Iso-Butanol and Comparison with Cellulosic Ethanol and n-Butanol*”, Biofuels, Bioprod. Biorefin. 8, 30-48.
- [4] Braun-Unkhoff M., Hansen N., Methling T., Moshhammer K., Yang B., 2017: “*The Influence of iso-Butanol Addition to the Chemistry of Premixed 1,3-Butadiene Flames*”, Proc. Combust. Inst. 36, 1311-1319.
- [5] Hansen N., Braun-Unkhoff M., Kathrotia T., Lucassen A., Yang B., 2015: “*Understanding the Reaction Pathways in Premixed Flames Fueled by Blends of 1,3-Butadiene and n-Butanol*”, Proc. Combust. Inst. 35, 771-778.
- [6] Ratcliff A., Luecke J., Williams A., Christensen E., Yanowitz J., Reek A., McCormick R.L., 2013: “*Impact of Higher Alcohols Blended in Gasoline on Light-Duty Vehicle Exhaust Emissions*”, Environ. Sci. Technol. 47, 13865-13872.
- [7] Böhm H., Braun-Unkhoff M., 2008: “*Numerical study on the effect of oxygenated blending compounds soot formation in shock tubes*”, Combust. Flame 153, 84-96
- [8] ASTM International ASTM D7862-13, 2013: “*Standard Specification for Butanol for Blending with Gasoline for Use as Automotive Spark-Ignition Engine Fuel*”, September 27, 2013:
- [9] Braun-Unkhoff M., Dembowski J., Herzler J., Karle J., Naumann C., Riedel U., 2014: “*Alternative Fuels based on Biomass: An experimental and modeling study of ethanol co-firing to natural gas*”, J. Eng. Gas Turbines Power 137(9), 091503-091503-9, GTP-14-1640, doi: 10.1115/1.4029625.
- [10] Herzler J., Herbst J., Kick Th., Naumann C., Braun-Unkhoff M., Riedel U., 2012: “*Alternative fuels based on biomass: an investigation on combustion properties of product gases*”, J. Eng. Gas Turbines Power, 135 (3), 031401-031401-9, GTP-12-1382.

- [11]Methling, T., Braun-Unkhoff M., Riedel U, 2013: “*A chemical-kinetic Investigation of Combustion Properties of Alternative Fuels - a Step towards a more efficient Power Generation*”, Proc. GT2013, ASME Turbo Expo 2013, San Antonio (USA), GT2013-64994.
- [12]Hohloch M., Widenhorn A., Lebküchner D., Panne T., Aigner M. 2008: “*Micro gas turbine test rig for hybrid power plant application*”, Proc. GT2008, ASME Turbo Expo 2008, Berlin (Germany), GT2008-50443.
- [13]Veloo P.S., Wang Y.L., Egolfopoulos F.N., Westbrook C.K., 2010: “*A comparative experimental and computational study of methanol, ethanol, and n-butanol flames*”, Combust. Flame 157(10), 1989-2004.
- [14]Sarathy S.M., Thomson M.J., Togbé C., Dagaut P., Halter F., Mounaim-Rousselle C., 2009: “*An experimental and kinetic modeling study of n-butanol combustion*”, Combust. Flame 156(4), 852-864.
- [15]Liu W., Kelley A.P., Law C.K., 2011: “*Non-premixed ignition, laminar flame propagation, and mechanism reduction of n-butanol, iso-butanol, and methyl butanoate*”, Proc. Combust. Inst. 33(1), 995-1002.
- [16]Wu F., Law C.K., 2013: “*An experimental and mechanistic study on the laminar flame speed, Markstein length and flame chemistry of the butanol isomers*”, Combust. Flame 160(12), 2744-2756.
- [17]Beeckmann J., Cai L., Pitsch H., 2014: “*Experimental investigation of the laminar burning velocities of methanol, ethanol, n-propanol, and n-butanol at high pressure*”, Fuel 117(A), 340-350.
- [18]Knorsch T., Zackel A., Mamaikin D., Zigan L., Wensing M., 2014: “*Comparison of Different Gasoline Alternative Fuels in Terms of Laminar Burning Velocity at Increased Gas Temperatures and Exhaust Gas Recirculation Rates*”, Energy Fuels 28(2), 1446-1452.
- [19]Broustail G., Seers P., Halter F., Moréac G., Mounaim-Rousselle C., 2011: “*Experimental determination of laminar burning velocity for butanol and ethanol iso-octane blends*”, Fuel 90(1), 1-6.
- [20]Li Q., Hu E., Cheng Y., Huang Z., 2013: “*Measurements of laminar flame speeds and flame instability analysis of 2-methyl-1-butanol–air mixtures*”, Fuel 112, 263-271.
- [21]Gu X., Huang Z., Li, Tang C., 2009: “*Measurements of Laminar Burning Velocities and Markstein Lengths of n-Butanol–Air Premixed Mixtures at Elevated Temperatures and Pressures*”, Energy Fuels 23 (10), 4900-4907.

- [22] Broustail G., Halter F., Seers P., Moréac G., Mounaim-Rousselle C., 2013: “*Experimental determination of laminar burning velocity for butanol/iso-octane and ethanol/iso-octane blends for different initial pressures*”, Fuel 106, 310-317.
- [23] Gu X., Huang Z., Wu S., Li Q., 2010: “*Laminar burning velocities and flame instabilities of butanol isomers-air mixtures*”, Combust. Flame 157(12), 2318-2325.
- [24] Zhu Y., Davidson D.F., Hanson R.K., 2014: “*1-Butanol ignition delay times at low temperatures: An application of the constrained-reaction-volume strategy*”, Combust. Flame 161(3), 634-643.
- [25] Heufer K.A., Fernandes R.X., Olivier H., Beeckmann J., Röhl O., Peters N., 2011: “*Shock tube investigations of ignition delays of n-butanol at elevated pressures between 770 and 1250 K*”, Proc. Combust. Inst. 33(1), 359-366.
- [26] Vranckx S., Heufer K.A., Lee C., Olivier H., Schill L., Kopp W.A., Leonhard K., Taatjes C.A., Fernandes R.X., 2011: “*Role of peroxy chemistry in the high-pressure ignition of n-butanol – Experiments and detailed kinetic modelling*”, Combust. Flame 158(8), 1444-1455.
- [27] Stranic I., Chase D.P., Harmon J.T., Yang S., Davidson D.F., Hanson R.K., 2012: “*Shock tube measurements of ignition delay times for the butanol isomers*”, Combust. Flame 159(2), 516-527.
- [28] Noorani K.E., Akih-Kumgeh B., Bergthorson J.M., 2010: “*Comparative High Temperature Shock Tube Ignition of C1-C4 Primary Alcohols*”, Energy Fuels 24 (11), 5834-5843.
- [29] Zhang J., Pan L., Gong J., Huang Z., Law C.K., 2013: “*A shock tube and kinetic modeling study of n-butanol oxidation*”, Combust. Flame 160(9), 1541-1549.
- [30] Black G., Curran H.J., Pichon S., Simmie J.M., Zhukov V., 2010: “*Bio-butanol: Combustion properties and detailed chemical kinetic model*”, Combust. Flame 157(2), 363-373, <http://c3.nuigalway.ie/biobutanol.html>.
- [31] Moss J.T., Berkowitz A.M., Oehlschlaeger M.A., Biet J., Warth V., Glaude P.-A., Battin-Leclerc F., 2008: “*An Experimental and Kinetic Modeling Study of the Oxidation of the Four Isomers of Butanol*”, J. Phys. Chem. A 112(43), 10843-10855.
- [32] POLIMI, HT-mech, Creck modeling group, Ranzi E., Faravelli, T., and co-workers, access 2016-nov-18, <http://creckmodeling.chem.polimi.it/index.php/menu-kinetics/menu-kinetics-detailed-mechanisms/menu-kinetics-prf-pah-alcohols-ethers-mechanism> .
- [33] Sarathy S.M., Vranckx S., Yasunaga K., Mehl M., Oßwald P., Metcalfe W.K., Westbrook C.K., Pitz W.J.,

- Kohse-Höinghaus K., Fernandes R.X., 2012: “*A comprehensive chemical kinetic combustion model for the four butanol isomers*”, *Combust. Flame* 159, 2028-2055, <https://combustion.llnl.gov/mechanisms/alcohols/butanol-isomers>.
- [34] Frassoldati A., Grana R., Faravelli T., Ranzi E., Oßwald P., Kohse-Höinghaus K., 2012: “*Detailed kinetic modeling of the combustion of the four butanol isomers in premixed low-pressure flames*”, *Combust. Flame* (159) 2295-2311.
- [35] Frassoldati A., Cuoci A., Faravelli T., Ranzi E., 2010: “*Kinetic modeling of the oxidation of ethanol and gasoline surrogate mixtures*”, *Combust. Sci. Technol.* (182) 653-667, doi: 10.1080/00102200903466368.
- [36] Frassoldati A., Cuoci A., Faravelli T., Niemann U., Ranzi E., Seiser R., Seshadri K. 2010: “*An experimental and kinetic modeling study of n-propanol and iso-propanol combustion*” *Combust. Flame* 157, 2-16.
- [37] Goldaniga A., Faravelli T., Ranzi E., Dagaut P., Cathonnet M., 1998: “*Oxidation of oxygenated octane improvers: MTBE, ETBE, DIPE, and TAME*”, *Proc. Combust. Inst.* 27, 353-360.
- [38] Goodwin D.G., Moffat H.K., Speth R.L., 2016: “*Cantera: An object-oriented software toolkit for chemical kinetics, thermodynamics, and transport processes*”, <http://www.cantera.org>, Version 2.2.1.
- [39] Kee R.J., Dixon-Lewis G., Warnatz J., Coltrin M.E., Miller J.A., 1986, “*The Chemkin Transport Database. Report SAND86-8246*”, Sandia National Laboratories, Livermore (CA), USA.
- [40] Kee R.J., Rupley F.M., Miller J.A., 1987, “*CHEMKIN: The Chemkin Thermodynamic Database. Rep. SAND87-8215*”, Sandia National Laboratories, Livermore (CA), USA.
- [41] Kee, R.J., Rupley, F.M. and Miller, J.A., “*Chemkin II: A FORTRAN Chemical Kinetics Package for the Analysis of Gas Phase Chemical Kinetics*”, Sandia Laboratories Report, SAND89-8009B.
- [42] Herzler J. and Naumann C., 2008: “*Shock Tube Study of the Ignition of Lean CO/H₂ Fuel Blends at Intermediate Temperatures and High Pressure*”, *Comb. Sci. Technol.* 180(10) 2015-2028.
- [43] Green W.H., Allen J.W., Beat A., Buesser R., Ashcraft W., Beran G.J., Class C.A., Gao C., Goldsmith C.F., Harper M.R., Jalan A., Keceli M., Magoon G.R., Matheu D.M., Merchant S.S., Mo J.D., Petway S., Raman S., Sharma S., Song J., Suleymanov Y., Geem K.M.V., Wen J., West R.H., Wong A., Wong H.W., Yelvington P.E., Yee N., Yu J., 2013: “*RMG-Reaction Mechanism Generator v4.0.1*”, <http://rmg.sourceforge.net>.
- [44] Slavinskaya N., Riedel U., Saibov E., Herzler J., Naumann C., 2014: “*Kinetic Surrogate Model for GTL*”

- Kerosene*”, Proc. 52nd AIAA Aerospace Sciences Meeting and Exhibit, No. AIAA 2014-0126.
- [45] Methling T., Braun-Unkhoff M., Riedel U., 2016: “*A novel linear transformation model for the analysis and optimisation of chemical kinetics*”, Combust. Theor. Model. 21(3), 503-528, doi 10.1080/13647830.2016.1251616
- [46] Herzler J. and Naumann C., 2009: “*Shock-tube study of the ignition of methane / ethane / hydrogen mixtures with hydrogen contents from 0 to 100% at different pressures*”, Proc. Combust. Inst. 32, 213-220.
- [47] Kick Th., Kathrotia T., Braun-Unkhoff M., Riedel U., 2011: “*An experimental and modeling study of laminar flame speeds of alternative aviation fuels*”, Proc. GT2011, ASME Turbo Expo, Vancouver, Canada, GT2011-45606.
- [48] Kick Th., Herbst J., Kathrotia T., Marquetand J., Braun-Unkhoff M., Naumann C., Riedel U., 2012: “*An Experimental and Modeling Study of Burning Velocities of Possible Future Synthetic Jet Fuels*”, Energy 43(1), 111-123.
- [49] Mzè Ahmed A., Dagaut P., Hadj-Ali K., Dayma G., Kick Th., Herbst J., Kathrotia T., Braun-Unkhoff M., Herzler J., Naumann C., Riedel U., 2012: “*Oxidation of a Coal-to-Liquid Synthetic Jet Fuel: Experimental and Chemical Kinetic Modeling Study*”, Energy Fuels, 26(10), 6070–6079, DOI: 10.1021/ef3009585.
- [50] Dagaut P., Karsenty F., Dayma G., Diévar P., Hadj-Ali K., Mzè-Ahmed A., 2013: “*Experimental and Detailed Kinetic Model for the Oxidation of a Gas to Liquid (GtL) Jet Fuel*”, Combust. Flame 161(3), 835-847, DOI: 10.1016/j.combustflame.2013.08.015.
- [51] Andrews G.E. and Bradley D., 1972: “*Determination of Burning Velocities: A Critical Review*”, Combust. Flame 18(1), 133-153.
- [52] Eberius H. and Kick Th., 1992: “*Stabilization of premixed, conical methane flames at high pressure*”, Ber. Bunsenges. Phys. Chem. 96(10), 1416-1419.

Table 1 Overview of measured laminar flame speeds of *n*-butanol-oxidizer mixtures; methods applied: c. flow: counterflow; c.v. bomb: combustion vessel (bomb).

T/K	$p / \text{bar or atm}^*$	ϕ	Method	Ref.
343	1	0.7-1.5	c. flow	Veloo [13]
350	0.89 *	0.8-1.2	c.v. bomb	Sarathy [14]
353	1; 2 *	0.7-1.4	c.v. bomb	Liu [15]
353; 373	1; 2; 5 *	0.7-1.4	c.v. bomb	Wu [16]
373	10	0.7-1.3	c.v. bomb	Beeckmann [17]
373; 423	1	0.7-1.5	heat flux	Knorsch [18]
393	1	0.8-1.4	c.v. bomb	Broustail [19]
393	1	0.7-1.8	c.v. bomb	Li [20]
413; 443; 473	1; 2.5	0.8-1.6	c.v. bomb	Gu [21]
423	1; 3; 5; 10	0.7-1.4	c.v. bomb	Broustail [22]
428	1; 2.5; 5; 7.5	0.7-1.5	c.v. bomb	Gu [23]

Table 2 Overview of measured ignition delay times of *n*-butanol-oxidizer mixtures (shock tube).

T/K	$p / \text{bar or atm}^*$	ϕ	Ref.
716-1121	20; 40 *	0.5, 1, 2	Zhu [24]
770-1250	10-42	1	Heufer [25]
795-1200	61-92	1	Vranckx [26]
1050-1600	1.5-43 *	0.5-1	Stranic [27]
1070-1760	2; 10; 12 *	0.5, 1, 2	Noorani [28]
1000-1650	1.3; 5; 10 *	0.5, 1, 2	Zhang [29]
1100-1800	1; 2.6; 8 *	0.5, 1, 2	Black [30]
1200-1800	1-4	0.25-1.0	Moss [31]

Table 3 Fuel-air mixtures studied in present work.

Mixture	Parameter range		
	Equivalence ratio ϕ	p / bar	T / K
A. Ignition delay time			
6750 ppm <i>n</i> -butanol	1.0	1	1400-1700
40498 ppm O ₂	1.0	4	1050-1550
952752 ppm Ar	1.0	16	950-1400
B. Burning velocity: Preheat temperature $T = \text{constant}$			
Composition given in mole fraction for $\phi = 1.0$			
0.03382 <i>n</i> -butanol	0.5 – 2.0	1	473
0.2029 O ₂	0.6 – 1.9	3	473
0.7633 N ₂	0.7 – 1.8	6	473

Table 4 Detailed chemical kinetic reaction models used.

Reference	Species	Reactions
DLR, present work		
<i>Detailed</i>	181	4567
<i>n</i> -butanol sub model	66	3749
hydrocarbon model (PRF)	115	818
<i>Reduced</i>	133	1182
<i>n</i> -butanol sub model	31	515
hydrocarbon model (PRF)	102	651
Black <i>et al.</i> [30]	243	2854
POLIMI_HT [32]	225	7645
Sarathy <i>et al.</i> [33]	426	2335

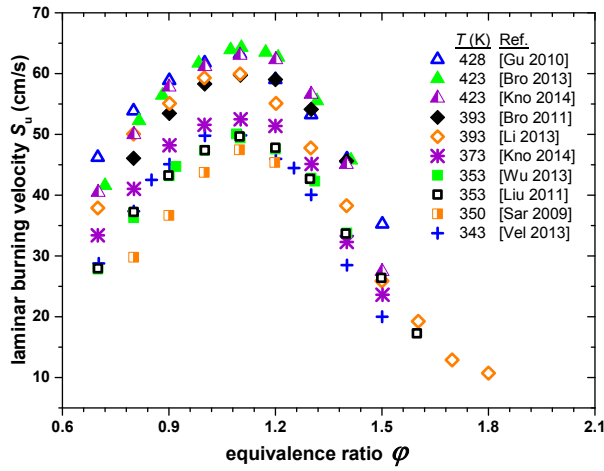


Fig. 1: Comparison of laminar flame speeds (n-butanol-air) at about $p = 1$ bar and at various preheat temperatures T [13-23]

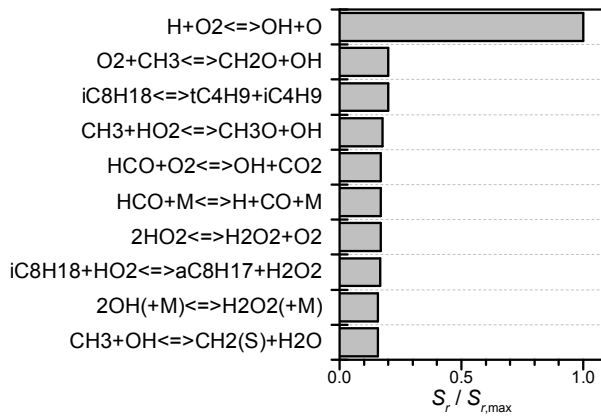


Fig. 2: Global sensitivity analysis of the detailed reaction mechanism (10 most important reactions)

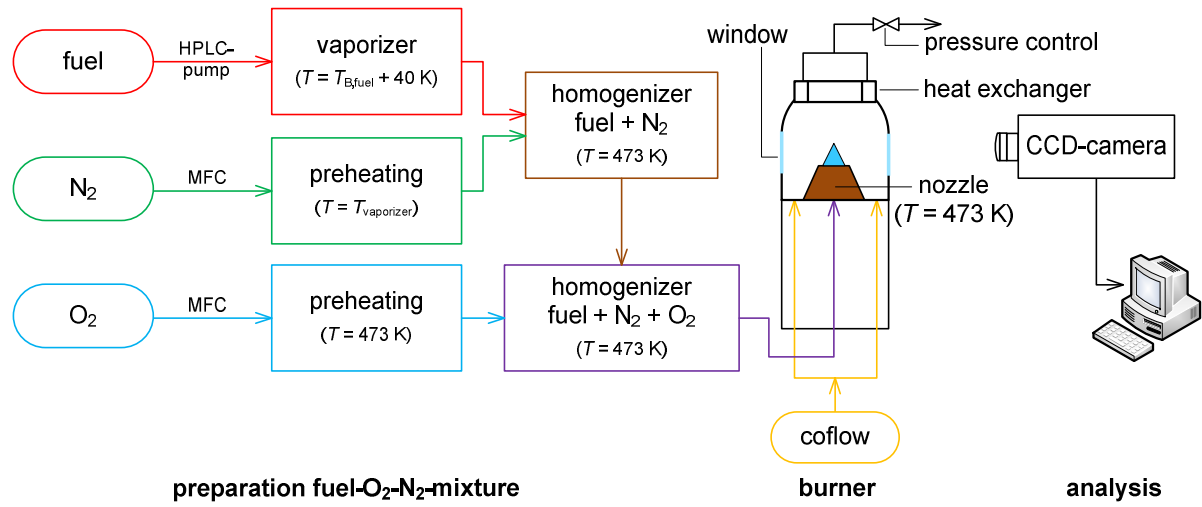


Fig. 3: Experimental setup of the burner system (MFC - mass flow controller; T_B - boiling point)

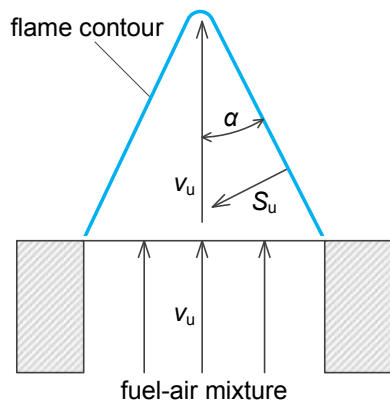


Fig. 4: Determination of the laminar burning velocity S_u (v_u - flow speed of the unburned gas mixture, α - cone angle)

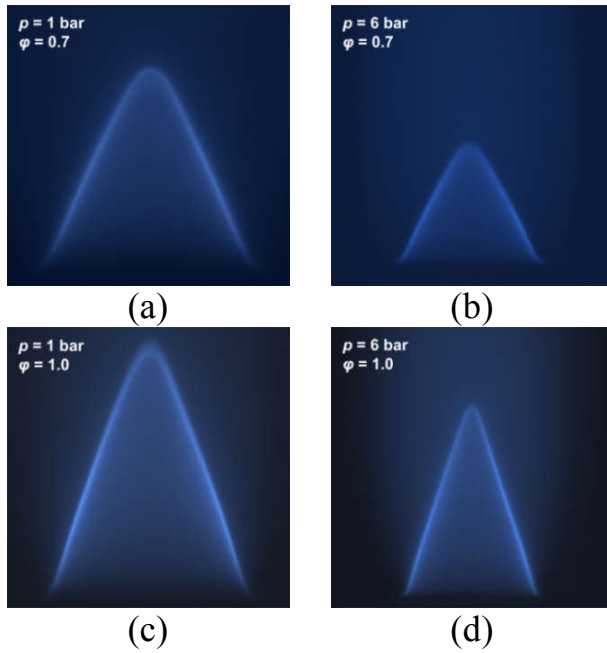


Fig. 5: Typical premixed *n*-butanol-air flames at $T = 473$ K and $p = 1$ bar (left) and $p = 6$ bar (right), for different φ -values: 0.7 (top) and 1.0 (bottom)

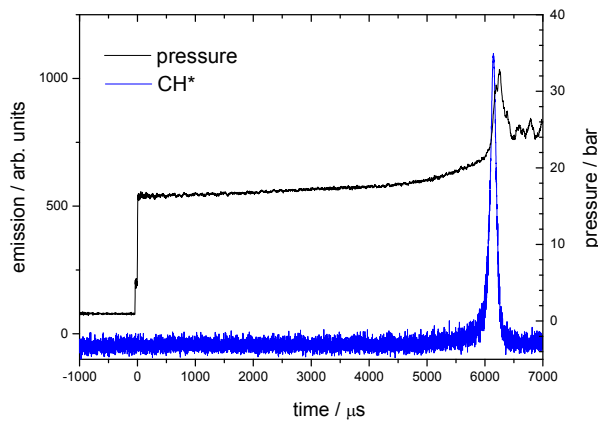


Fig. 6: Pressure and emission signals: *n*-butanol / O_2 / Ar sample; $\varphi = 1.0$, $p = 16.3$ bar; $T = 990$ K; dilution (Ar) 1:5;

$$\tau_{\text{ign}} = 6155 \mu\text{s}$$

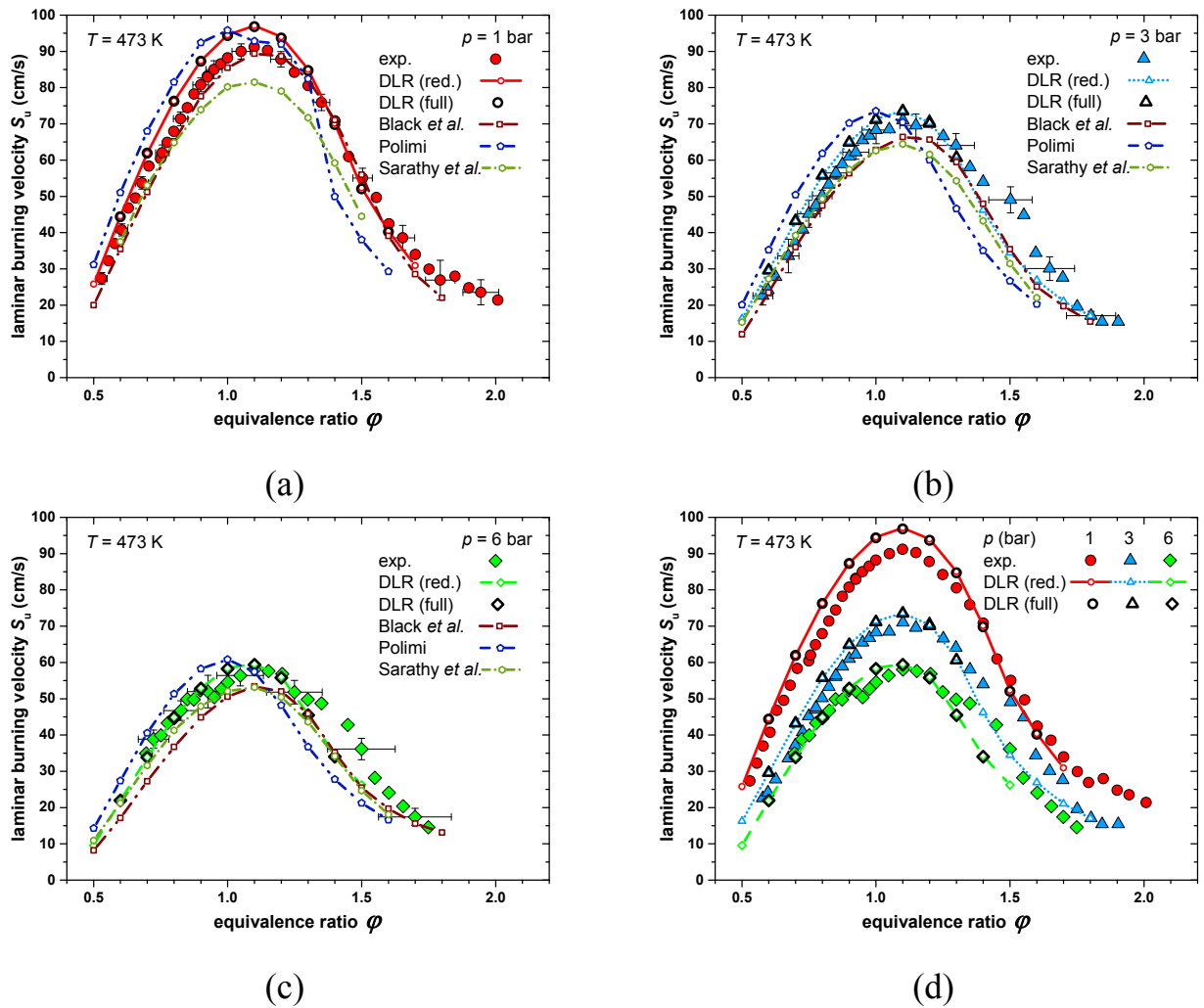


Fig. 7: Comparison between measured burning velocities (full symbols) and calculated laminar flame speeds (curves, open symbols) of n -butanol-air mixtures: $T = 473$ K for $p = 1$ bar, 3 bar, and $p = 6$ bar

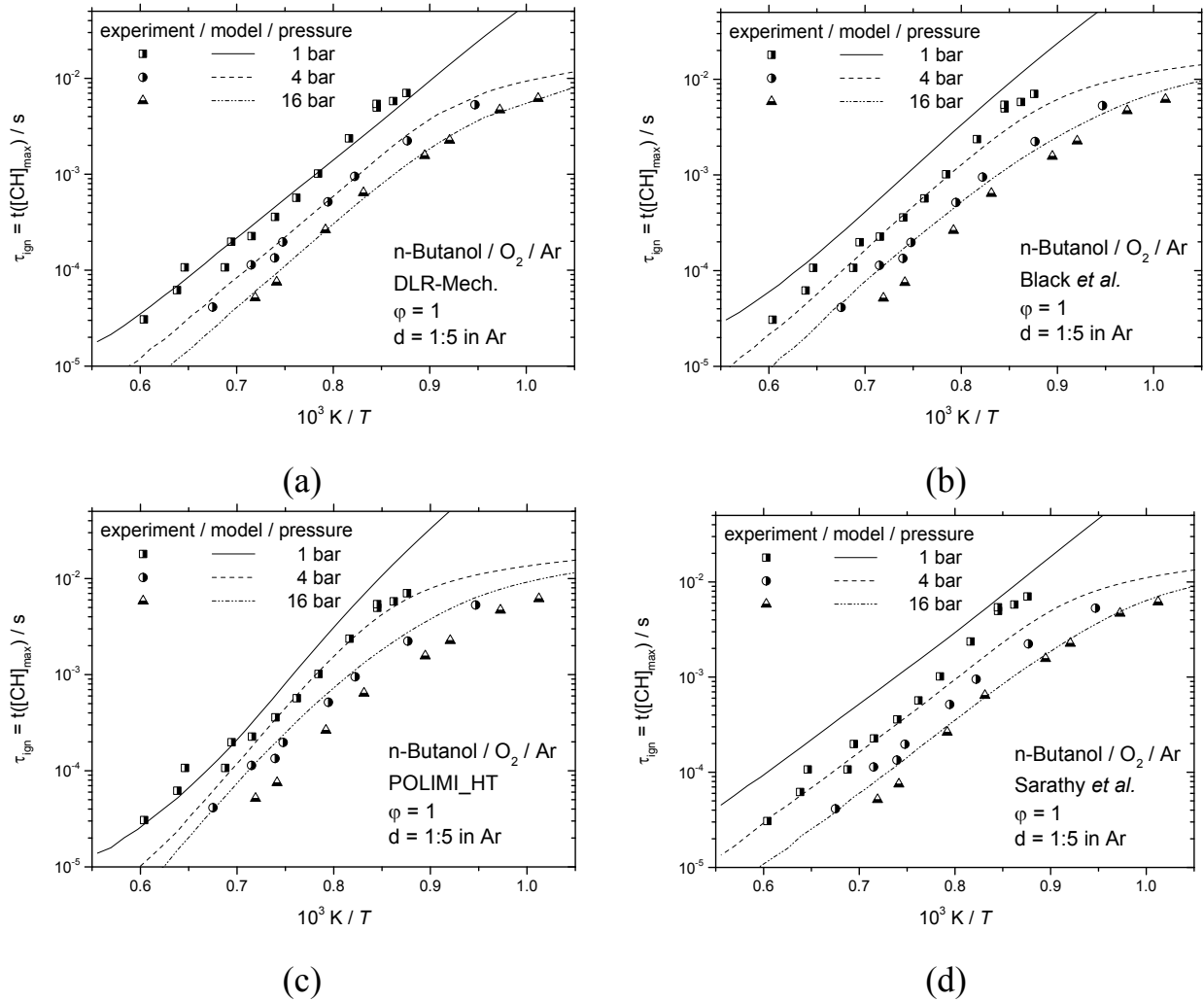


Fig. 8. Comparison between measured (circles - full symbols) and calculated ignition delay times (curves, open symbols) of *n*-butanol-O₂-Ar mixtures

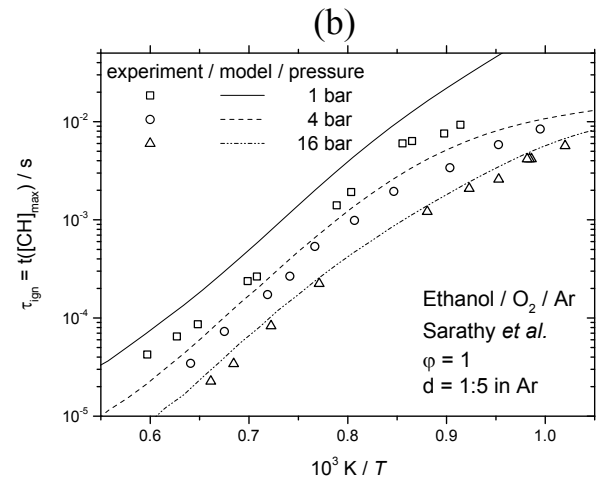
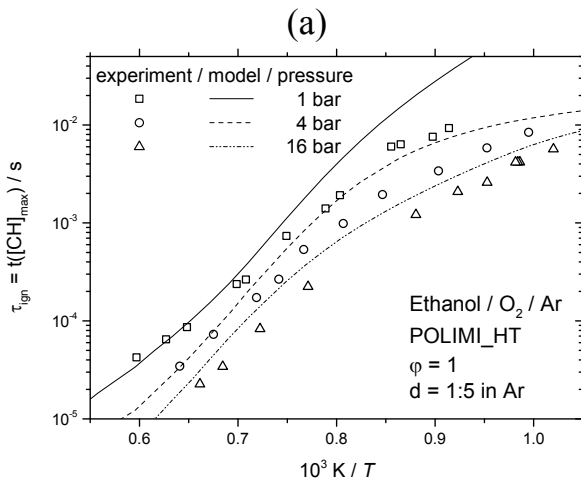
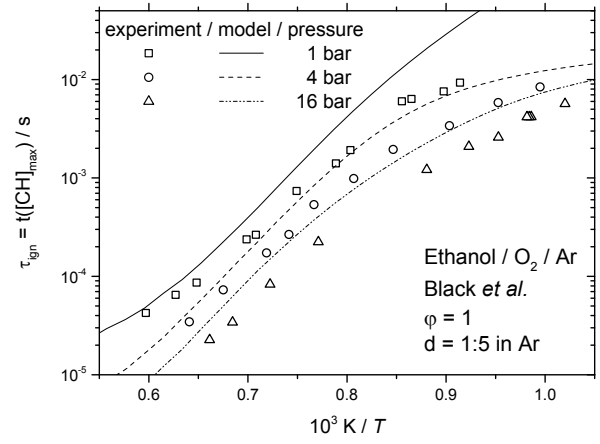
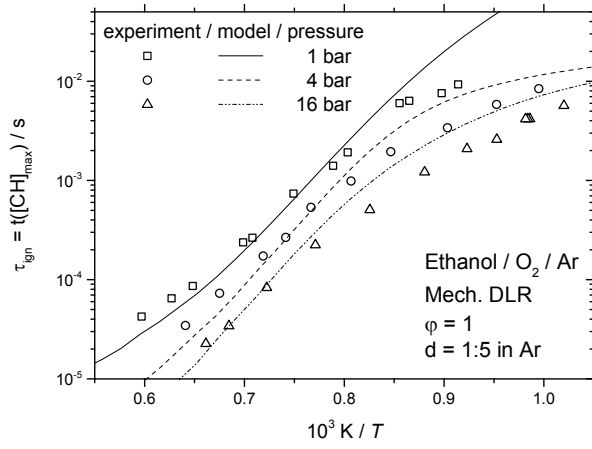


Fig. 9: Comparison between measured (circles - full symbols) and calculated ignition delay times (curves, open symbols) of *n*-ethanol-O₂-Ar mixtures

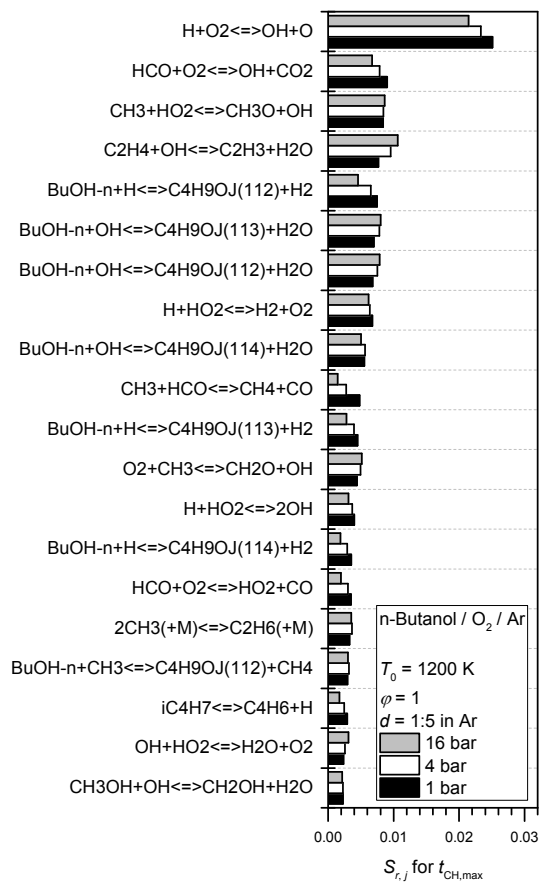


Fig. 10: Sensitivity of ignition delay time